

# S-, C- and L-Band Photonic Integrated Wavelength Selective Switch

R. Kraemer<sup>(1)</sup>, F. Nakamura<sup>(2)</sup>, H. Tsuda<sup>(2)</sup>, A. Napoli<sup>(3)</sup>, Calabretta<sup>(1)</sup>

<sup>(1)</sup>IPI-ECO Research Institute, Eindhoven University of Technology, Eindhoven, the Netherlands, [r.magalhaes.gomes.kraemer@tue.nl](mailto:r.magalhaes.gomes.kraemer@tue.nl).

<sup>(2)</sup>Graduate School of Science and Technology, Keio University, Yokohama, Japan.

<sup>(3)</sup>Infinera, Germany.

**Abstract** A photonic integrated WSS operating on the S-, C- and L-Band is presented with an average extinction-ratio of -20.40 dB. Crosstalk levels were kept below -20 dB for all bands and experimental results on NRZ OOK data indicate error-free operation for up to 35 Gb/s.

## Introduction

It is predicted that IP traffic demand in metro and *data center interconnects* (DCI) will continue to significantly grow on a yearly basis<sup>[1]</sup>. Thus, currently deployed optical systems – operating on the C-Band only – will no be any longer capable of supporting the current exponential bandwidth demand growth. Several approaches have been proposed to boost the throughput of optical systems, among them: *spatial division multiplexing* (SDM), *multi-core/mode fiber* (MMF/MCF), *multi-band transmission* (MBT). Recent studies<sup>[2],[3]</sup> show that MBT systems, using the full low loss spectrum of optical fibers, i.e., from the O- to the L-band (1260 nm - 1625 nm), may provide a gain factor of up to 10× when compared to C-Band only systems.

As optical commercial systems move toward MBT<sup>[4]</sup>, the management of such a wide spectrum is expected to become a relevant. In this context, the *Wavelength Selective Switch* (WSS) – a device capable of routing each channel ( $\lambda$ ) injected into a common port to any of its  $N$  output ports – is one of the enabling modules to realize MBT. High port-count WSS are typically based on free-space optics and *micro-electromechanical systems* (MEMS) or *liquid crystal on silicon* (LCOS) that make these devices bulky and costly due to the high precision required on its assembly<sup>[5]</sup>. On the other hand, WSS based on integrated photonics are compact and a potential low-cost alternative for edge access or networks residing closer to the end user, where there is less need for multi-degree optical mesh connectivity, yet with the full flexibility of the higher degree configurations<sup>[6],[7]</sup>. Commercial MBT systems are already targeting the upgrade of existing C-band systems, first on the C+L configuration, by capitalizing the amplification available at this part of the spectrum<sup>[4],[8]</sup>.

Furthermore, recent research have been also using the S-band part of the spectrum to achieve record-breaking data transmission<sup>[9]–[11]</sup>. Thus, novel WSS operating on the S-, C- and L-bands are especially important. High cost C+L WSS based on LCOS have been reported<sup>[12]</sup> as well as photonic integrated WSS based on microring resonators that required active tuning to operate on the C or L-band<sup>[13]</sup>. In this work we report for the first time, to the best of our knowledge, a novel photonic integrated  $1 \times 2$  WSS operating simultaneously on the S-,C- and L-bands with a total of 109 controllable channels. We report an average *extinction-ratio* (ER) of -20.40 dB across all bands and crosstalk is kept below -20 dB. Experimental results also show error-free operation with limited penalty at 10 Gb/s at the S-band and also error free at the C and L-Bands for bit-rates up to 35 Gb/s with limited penalty.

## $1 \times 2$ Photonic Integrated WSS

Fig. 1 shows the layout of the fabricated WSS. The photonic integrated WSS is a  $1 \times 2$  device, and designed as 40 Channel device with 100 GHz channel spacing on the C-band with no waveguide crossings. The WSS uses  $1.5\% \Delta$  silica waveguides on a silicon substrate and it consists of a demultiplexer *arrayed-waveguide grating* (AWG), a switching section and a multiplexer AWG. By employing a loop-back scheme that unifies the two AWGs eventual mismatches between center wavelengths of the WSS are eliminated. The switching section consists of single-stage *Mach-Zehnder Interferometers* (MZIs) with two arms of equal length and thermo-optic phase shifters and MZIs with two arms of different lengths as wavelength couplers. Further details on the fabricating and a characterization on the C-band may be found on<sup>[14]</sup>. The WSS if fully

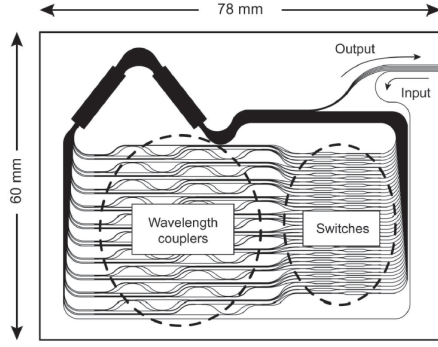


Fig. 1: WSS Layout

packaged and pigtailed with an embedded switch controller for selecting each of the MBT channels.

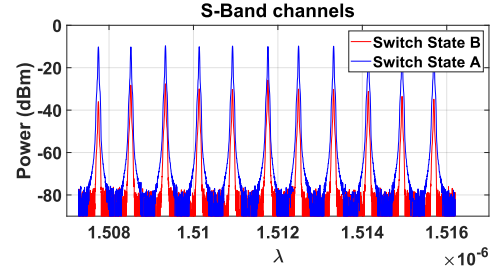
It is known<sup>[15]</sup> that the spatial dispersion of an AWG is determined by the order of the array,  $m$ , and the divergence angle between waveguides,  $\Delta\alpha$ . If the change in the input wavelength is such that the phase difference has increased by  $2\pi$ , the transfer to the output of the array will occur, meaning that the AWG response is periodic. This periodicity on the frequency domain is called the *Free Spectral Range* (FSR) and is given by:

$$FSR = \frac{\nu_c}{m} \left( \frac{n_{eff}}{n_g} \right) \quad (1)$$

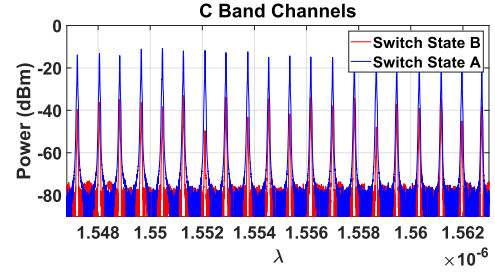
where  $\nu_c$  is the frequency of the propagating wave,  $n_{eff}$  the effective refractive index of the guided mode and  $n_g$  is the group index. Fig. 2 shows the contrast ratio between switch states for some of the channels on the S, C and L-bands. In this figure the blue line is the channel at the output A of the device when no control signals are applied, and the red line is the channel, at the same output A, when switching occurs. In this device we have a total of 109 controllable channels across the multi-band spectrum (40 in the S-band from 1485 nm to 1516 nm, 40 in the C-band from 1532 nm to 1564 nm and 29 in the L-band from 1583 nm to 1609 nm). We found average ERs of -18.21 dB, -22.59 dB and -19.39 dB, and crosstalk levels below -22 dB, -26 dB and -20 dB at the S-, C- and L-band, respectively.

### Experimental results and Discussion

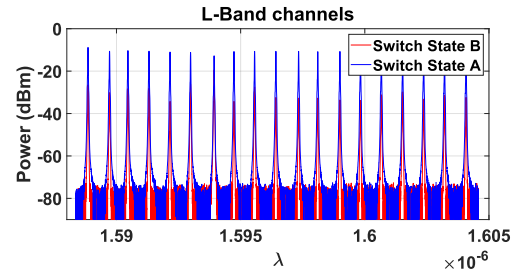
The experimental setup depicted on Fig. 3 was used to assess the *bit-error-rate* (BER) performance of the WSS. For the C and L-bands, a broadband *tunable laser source* (TLS) covering them was used to generate a *continuous-wave* (CW) optical signal. After the CW source a *polarization controller* (PC) was used to optimize the *state-of-polarization* (SOP) for the optical modulator, which in turn was driven at 10 Gb/s or 35



(a) S-Band contrast ratio.



(b) C-Band contrast ratio.



(c) L-Band contrast ratio.

Fig. 2: Contrast Ratio for S (2a), C (2b) and L-Bands (2c).

Gb/s non-return zero on-off keying (NRZ OOK) data with a pattern length of  $2^{31} - 1$ . After the modulator, an *erbium-doped-fiber-amplifiers* (EDFAs) operating on the C or L-band were used to compensate the 14 dB losses introduced by the modulator. After the EDFA another PC was used to control the SOP for the polarization sensitive WSS. In Figs. 3b and 3c we can see the *optical signal-to-noise-ratio* (OSNR) at both outputs of the device for channels on C and L-band. The measured OSNRs at both outputs were  $\geq 47$  dB.

Figs. 4b, 4c, 4d and 4e show the BER performance across the C and L-bands for single channels at 10 Gb/s and 35 Gb/s. The controlling of each channel is similar across the entire spectrum, with control signals being applied to the MZI phase shifter where the given channel is propagating. At 10 Gb/s the power penalty at  $10^{-9}$  is around 0.5 dB at the output B and negligible at the L-Band at output A. For 35 Gb/s the penalty was up to 2 dB at the C-Band at the output B, and ranging from 0.5 dB to 3.5 dB at the L-Band at output A. This penalty increase

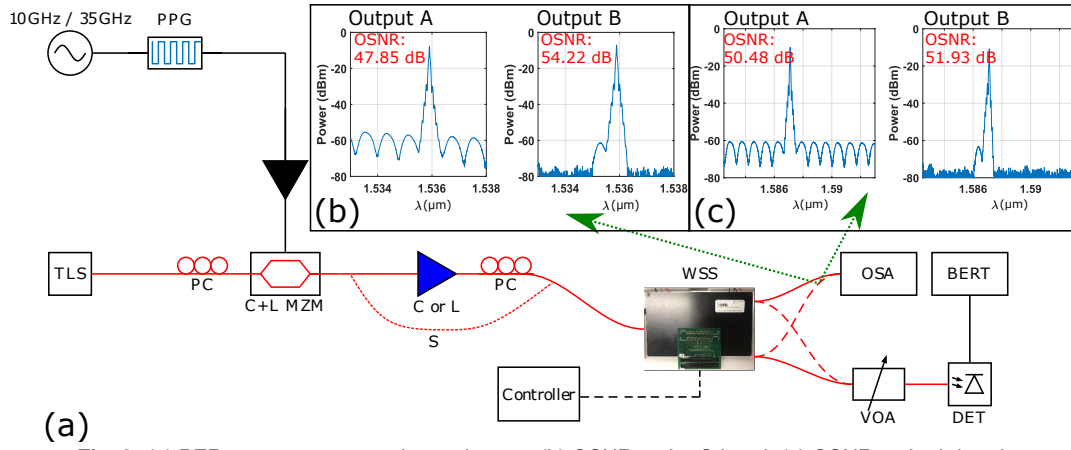


Fig. 3: (a) BER assessment experimental setup. (b) OSNR at the C-band. (c) OSNR at the L-band.

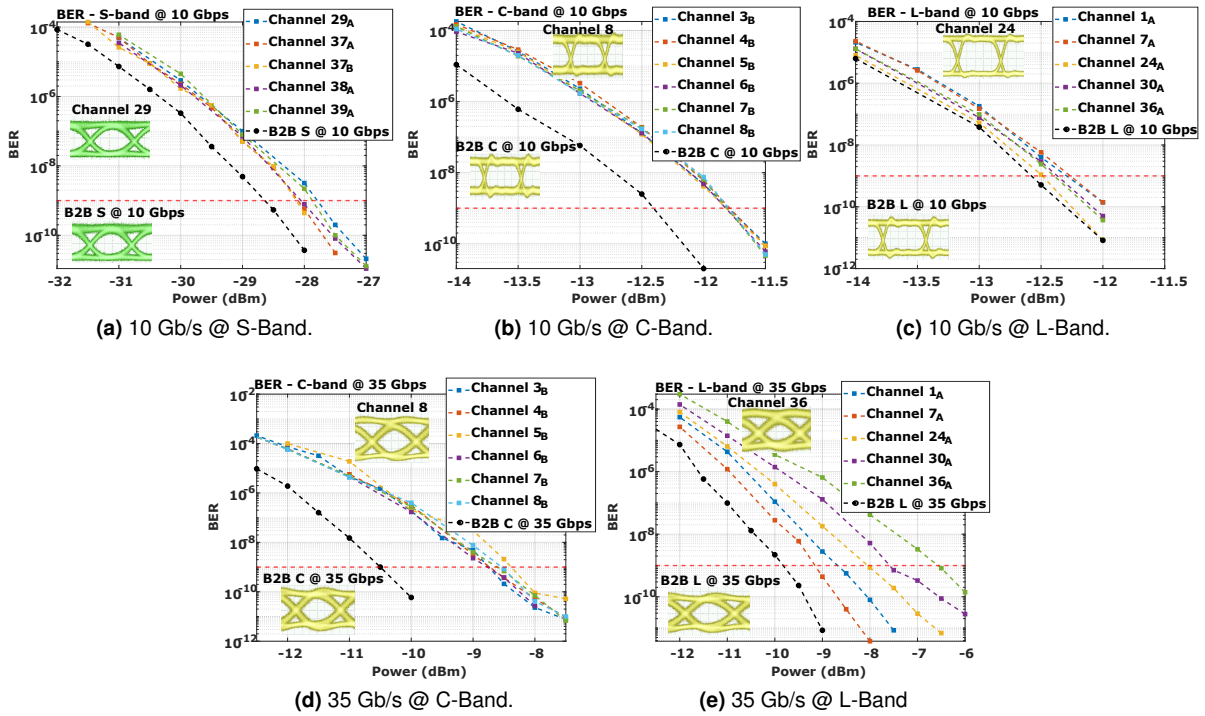


Fig. 4: BER results for the S-, C- and L-band.

at L-band, specially for longer wavelengths, can be explained by analyzing the narrower channels at longer wavelengths (0.8 nm at 1550 nm vs  $\sim 0.7$  nm at 1600 nm) which in turn translates to a reduction of the 3dB bandwidth, which is  $\sim 36$  GHz at the C-band<sup>[14]</sup>.

In order to assess the performance within the S-band, the experimental setup of Fig. 3 was used but without the optical amplifier after the modulator, as we lacked means of amplification at this band. In light of this, a high-sensitivity APD, limited to 10 Gb/s, was used for detecting the signals. Error free operation is also obtained with a penalty of  $\sim 0.5$  dB at  $\text{BER} = 10^{-9}$ . In line with the BER results within C- and L-band, with an S-band amplifier, also error free operation at 35 Gb/s is expected.

## Conclusions

In this work we presented a  $1 \times 2$  photonic integrated WSS operating simultaneously at the S-, C- and L-band with 109 channels, average extinction ratio of -20.40 dB with crosstalk below -20 dB. Experimental results show error-free operation for all bands with limited penalty in both outputs. The multiband performance also shows that this device is a viable option for recently deployed C+L systems, and for the newly demonstrated S+C+L systems, specially in networks and scenarios with less need for multidegree optical mesh connectivity.

## Acknowledgements

This project has received funding from the European Union's Horizon 2020 research and innovation programme under the Marie Skłodowska-Curie grant agreement 814276.

## References

- [1] Cisco visual networking index: Forecast and methodology, 2017-2022, <https://www.cisco.com/c/en/us/solutions/collateral/executive-perspectives/annual-internet-report/white-paper-c11-741490.html>.
- [2] A. Ferrari, A. Napoli, J. K. Fischer, N. Costa, A. D'Amico, J. Pedro, W. Forsysiak, E. Pincemin, A. Lord, A. Stavdas, G. Roelkens, N. Calabretta, S. Abrate, B. Sommerkorn-Krombholz, and V. Curri, "Assessment on the Achievable Throughput of Multi-band ITU-T G.652.D Fiber Transmission Systems", en, *JOURNAL OF LIGHTWAVE TECHNOLOGY*, p. 14,
- [3] N. Sambo, A. Ferrari, A. Napoli, N. Costa, J. Pedro, B. Sommerkorn-Krombholz, P. Castoldi, and V. Curri, "PROVISIONING IN MULTI-BAND OPTICAL NETWORKS: A C+L+S-BAND USE CASE", en, p. 4,
- [4] V. Lopez, B. Zhu, D. Moniz, N. Costa, J. Pedro, X. Xu, A. Kumpera, L. Dardis, J. Rahn, and S. Sanders, "Optimized design and challenges for c l band optical line systems", *Journal of Lightwave Technology*, vol. 38, no. 5, pp. 1080–1091, 2020.
- [5] D. Marom, D. Neilson, D. Greywall, Chien-Shing Pai, N. Basavanthally, V. Aksyuk, D. Lopez, F. Pardo, M. Simon, Y. Low, P. Kolodner, and C. Bolle, "Wavelength-selective  $1 \times K$  switches using free-space optics and MEMS micromirrors: Theory, design, and implementation", en, *Journal of Lightwave Technology*, vol. 23, no. 4, pp. 1620–1630, Apr. 2005, ISSN: 0733-8724. DOI: 10.1109/JLT.2005.844213.
- [6] B. C. Collings and P. Roorda, "ROADM-Based Networks", en, in *Optically Amplified WDM Networks*, Elsevier, 2011, pp. 23–45, ISBN: 978-0-12-374965-9. DOI: 10.1016/B978-0-12-374965-9.10002-0.
- [7] Y. Ikuma, T. Mizuno, H. Takahashi, T. Ikeda, and H. Tsuda, "Low-loss Integrated  $1 \times 2$  Gridless Wavelength Selective Switch With a Small Number of Waveguide Crossings", en, in *European Conference and Exhibition on Optical Communication*, Amsterdam: OSA, 2012, Tu.3.E.5, ISBN: 978-1-55752-950-3. DOI: 10.1364/ECEOC.2012.Tu.3.E.5.
- [8] J.-X. Cai, H. G. Batshon, M. V. Mazurczyk, O. V. Sinkin, D. Wang, M. Paskov, W. Patterson, C. R. Davidson, P. Corbett, G. Wolter, T. Hammon, M. Bolshtyansky, D. Foursa, and A. Pilipetskii, "70.4 Tb/s Capacity over 7,600 km in C+L Band Using Coded Modulation with Hybrid Constellation Shaping and Nonlinearity Compensation", en, in *Optical Fiber Communication Conference Postdeadline Papers*, Los Angeles, California: OSA, 2017, Th5B.2, ISBN: 978-1-943580-24-8. DOI: 10.1364/OFC.2017.Th5B.2.
- [9] L. Galdino, A. Edwards, W. Yi, E. Sillekens, Y. Wakayama, T. Gerard, W. S. Pelouch, S. Barnes, T. Tsuritani, R. I. Killey, D. Lavery, and P. Bayvel, "Optical Fibre Capacity Optimisation via Continuous Bandwidth Amplification and Geometric Shaping", en, *IEEE Photonics Technology Letters*, vol. 32, no. 17, pp. 1021–1024, Sep. 2020, ISSN: 1041-1135, 1941-0174. DOI: 10.1109/LPT.2020.3007591.
- [10] F. Hamaoka, M. Nakamura, S. Okamoto, K. Minoguchi, T. Sasai, A. Matsushita, E. Yamazaki, and Y. Kisaka, "Ultra-Wideband WDM Transmission in S-, C-, and L-Bands Using Signal Power Optimization Scheme", en, *Journal of Lightwave Technology*, vol. 37, no. 8, pp. 1764–1771, Apr. 2019, ISSN: 0733-8724, 1558-2213. DOI: 10.1109/JLT.2019.2894827.
- [11] J. Renaudier, A. Arnould, A. Ghazisaeidi, D. Le Gac, P. Brindel, E. Awwad, M. Makhsiyani, K. Mekhazni, F. Blache, A. Boutin, *et al.*, "Recent advances in 100+ nm ultra-wideband fiber-optic transmission systems using semiconductor optical amplifiers", *Journal of Lightwave Technology*, vol. 38, no. 5, pp. 1071–1079, 2020.
- [12] K. Seno, K. Yamaguchi, K. Suzuki, and T. Hashimoto, "Wide-Passband C+L-band Wavelength Selective Switch by Alternating Wave-Band Arrangement on LCOS", en, p. 3,
- [13] P. Prabhathan, Z. Jing, V. M. Murukeshan, Z. Huijuan, and C. Shiyi, "Discrete and Fine Wavelength Tunable Thermo-Optic WSS for Low Power Consumption C+L Band Tunability", en, *IEEE Photonics Technology Letters*, vol. 24, no. 2, pp. 152–154, Jan. 2012, ISSN: 1041-1135, 1941-0174. DOI: 10.1109/LPT.2011.2174979.
- [14] Y. Ikuma, T. Mizuno, H. Takahashi, and H. Tsuda, "Integrated  $40\text{-}\lambda$   $1 \times 2$  Wavelength Selective Switch Without Waveguide Crossings", en, *IEEE Photonics Technology Letters*, vol. 25, no. 6, pp. 531–534, Mar. 2013, ISSN: 1041-1135, 1941-0174. DOI: 10.1109/LPT.2013.2240291.
- [15] H. Venghaus, Ed., *Wavelength filters in fibre optics*, en, ser. Springer series in optical sciences 123. Berlin ; New York: Springer, 2006, ISBN: 978-3-540-31769-2.